

Viscoelasticity of mono- and polydisperse inverse ferrofluids

Ruben Saldivar-Guerrero,^{,§,¥} Reinhard Richter,^{*,§} Ingo Rehberg,[§] Nuri Aksel,[‡] Lutz Heymann[‡] and
Oliverio S. Rodriguez-Fernández[¥]*

[§] Experimentalphysik V, Universität Bayreuth, D-95440 Bayreuth, Germany

[‡] Lehrstuhl für Technische Mechanik und Strömungsmechanik, Universität Bayreuth, D-95440
Bayreuth, Germany

[¥] Centro de Investigación en Química aplicada, 25100 Saltillo, Coahuila México.

RECEIVED DATE

* CORRESPONDING AUTHORS E-Mail: rubensaldivar@terra.com.mx

reinhard.richter@uni-bayreuth.de

ABSTRACT. We report on measurements of a magnetorheological model fluid created by dispersing nonmagnetic microparticles of polystyrene in a commercial ferrofluid. The linear viscoelastic properties as a function of magnetic field strength, particle size and particle size distribution are studied by oscillatory measurements. We compare the results with a magnetostatic theory proposed by .J. De Gans, C. Blom, A. P. Philipse, and J. Mellema, Phys. Rev. E, **60**, 4518 (1999) for the case of gap spanning chains of particles. We observe these chain-structures via a long distance microscope. For monodisperse particles we find good agreement of the measured storage modulus with theory, even for an extended range, where the linear magnetization law is no longer strictly valid. Moreover we compare for the first

time results for mono- and polydisperse particles. For the latter, we observe an enhanced storage modulus in the linear regime of the magnetization.

1. Introduction

Common magnetorheological fluids (MRFs) are suspensions of *micron-sized*, magnetizable particles like carbonyl iron dispersed in a non-magnetic carrier liquid. They have the ability to change their rheological properties by the formation of aggregates under the influence of a magnetic field. Their shear behavior is typically described as that of a classical Bingham fluid, which is a material that does not flow unless the applied stress exceeds the yield stress. For MRFs, the yield stress is a function of the applied field strength [1].

Refining the size of the magnetizable particles to the range of 10 nm, one obtains ferrofluids [2]. They comprise magnetic monodomain particles, which are prevented from sticking together by surfactants (or electric charges) and more importantly, by a comparable value of their thermal energy. Due to this, the formation of aggregates is in ferrofluids much less important for the flow behavior, when compared to MRFs. Despite that, magnetorheology in dense ferrofluids has become a focus of research as well [3]. Recently, a molecular dynamics study of chain formation in ferrofluids uncovered, that a background of small particles diminishes the chain formation between the larger ones considerably [4].

However, for a comparison with theory, the size distribution needs to be precisely known. This problem is overcome in this article by investigating inverse ferrofluids. Since the early studies of Skjeltorp [5] it is known that plain ferrofluids can be transformed to MRFs by the suspension of non-magnetic particles, like micron-size polystyrene or silica spheres. These non-magnetic particles create holes which appear to possess a magnetic moment m , corresponding to the volume of the displaced fluid. Because monodisperse non-magnetic particles can be produced in different size with high accuracy, inverse ferrofluids are ideal model fluids for investigating the influence of particle size and particle size distribution on the magnetorheological effect.

The theories available to quantify a field dependent rheological effect predict that it should be independent of the particle size [6, 7, 8, 9, 10, 11]. However, they are assuming monodisperse particles.

Nonmagnetic particles used in most previous studies have been rather polydisperse [1, 12, 13]. Only recently, two studies have been put forward by de Gans et al., investigating the yield stress [11] and linear viscoelasticity [10] of monodisperse inverse ferrofluids. They have been utilizing silica spheres with mean radius ranging from 53 nm to 190 nm. In oscillatory measurements they found reasonable agreement with their model of linear viscoelasticity as long as the condition of isolated gap spanning chains is met.

We extend their studies by implementing monodisperse polystyrene spheres with diameters of 3 μm and 11 μm . Because of the suitable size of our nonmagnetic particles, we are able to observe a network of chains by video-microscopy. We find a convincing quantitative agreement with the above mentioned model [10]. Moreover we compare for the first time the magnetorheological properties of mono- and polydisperse particles suspended in a ferrofluid. In this way we are approaching the realistic situation for standard MRFs and ferrofluids. We observe stiffening in the linear regime of the magnetization due to the polydispersity. For larger magnetic fields the polydisperse fluid has a weaker storage modulus than the monodisperse one.

2. Theoretical background

De Gans et al. [10] developed a theory which describes the linear viscoelastic behavior of inverse fluids. For the derivation, they assume that the ferrofluid is magnetically continuous on the length scale of the radius of the nonmagnetic particles, which are spherical and monodisperse. In addition, the stress must be dominated by the contribution of the particle interactions in the chains, the interchain interactions are neglected, and the deformation of the chains under shear is affine. The magnetic moment of the void displaced by a particle is given

a) in the linear regime, i.e. for constant magnetic permeability, by

$$m = -4\pi\beta R^3 H. \quad (1)$$

b) in the saturated limit by

$$m = -\frac{4}{3} \pi R^3 M_S. \quad (2)$$

In both equations R denotes the radius of the spherical particles, H the magnetic field, M_S the saturation magnetization and β the effective permeability of the suspension according to

$$\beta = \frac{\mu_r - 1}{2\mu_r + 1}, \quad (3)$$

where μ_r represents the relative permeability of the ferrofluid.

A collection of identical holes will thus behave as a many-body system with dipolar interactions which may be controlled by an external field. The dipole-dipole energy between two particles is

$$U_d = \frac{\mu_0 \mu_r m^2}{4\pi r^3} (1 - 3 \cos^2 \theta). \quad (4)$$

Here m is the induced magnetic moment of the non-magnetic particles, described above, r the center-to-center distance between two particles, θ the angle between the applied field H and the center-to-center vector, and μ_0 the permeability of the vacuum. U_d becomes minimal for $\theta = 0$, i.e. for particles which align to chain like aggregates in direction of the magnetic field. The chain formation becomes increasingly important when the coupling parameter [13]

$$\lambda = \frac{U_d}{k_B T} \quad (5)$$

representing the ratio of the dipole-dipole energy to the thermal energy is larger than unity. The coupling parameter can be increased either by using a ferrofluid with a higher susceptibility or by using larger non-magnetic particles. Following de Gans *et al.* [11], the average length $\langle i \rangle$ of chains, which are formed due to the magnetic field, can be estimated according to

$$\langle i \rangle = \frac{2x}{\sqrt{1 + 4x - 1}}. \quad (6)$$

with

$$x = \frac{\phi_V e^{2\lambda}}{3\lambda^2} \left(2 + \frac{5}{\lambda} + \frac{10}{\lambda^2} \right), \quad (7)$$

where ϕ_v denotes the volume fraction of the nonmagnetic particles. An important limit is met if all chains percolate from the top plate to the bottom plate of the rheometer. The fraction of chains that is gap spanning can be approximated by

$$\tilde{N}_g = e^{-N_{\text{gap}}/\langle i \rangle}. \quad (8)$$

Here $N_{\text{gap}} = \delta/(2R)$ measures the gap δ of the rheometer in number of spheres of radius R , where $r = 2R$ is assumed. For particles in the micrometer range, one needs a rather weak magnetic field to fulfill $\tilde{N}_g \approx 1$, as will be discussed later (see Table 2 below). Then all chains are gap spanning and it can be seen, that indeed the particle size has no influence on the shear stress: The shear stress is proportional to the number N of particle chains per unit surface area A and to the force $\sim \partial U_d / \partial r$ acting on the chains

$$\sigma \sim \frac{N}{A} \frac{\partial U_d}{\partial r} \sim \frac{\phi_v}{R^2} \frac{m^2}{R^4} \sim \frac{\phi_v}{R^2} \frac{R^6}{R^4}. \quad (9)$$

Here we have taken advantage of Eq.(4) in connection with Eq. (1) or (2).

More thoroughly the storage modulus in the linear regime, i.e. for $m = -4\pi\beta R^3 H$, can be derived by calculating the stress on the chains of particles sheared between parallel plates perpendicular to the magnetic field. In this way the high frequency limit of the storage modulus is found to be [10]:

$$G'_\infty = \frac{3}{4} \mu_0 \mu_r \beta^2 \zeta(4) \phi_v H^2 \left[2 \left(1 + \frac{\beta \zeta(3)}{2} \right)^{-2} + \left(1 - \frac{\beta \zeta(3)}{4} \right)^{-2} \right]. \quad (10)$$

Here $\zeta(n)$ denotes the Riemann ζ function.

In this work we measure the storage modulus G' and loss modulus G'' of inverse ferrofluids using monodisperse and polydisperse polystyrene particles of different sizes in oscillatory measurements. We then compare the results with Eq. (10) proposed by de Gans *et al.* for the storage modulus.

3. Experimental

3.1 Materials. The nonmagnetic particles used in our experiments were monodisperse polystyrene particles of 3 and 11 μm in diameter, and polydisperse particles with a mean diameter of 1.08 μm supplied by Microbeads AS. The density of the particles is 1.05 g (ml)^{-1} . The particles were dried in a freeze dryer system and used without further treatment. The polystyrene particles observed by an optical microscope are shown in Fig. 1. The size distribution obtained by static light scattering is depicted in Fig. 2. The corresponding mean diameter and normalized polydispersity $I = (d_{90} - d_{10}) / d_{50}$ of the polystyrene particles are displayed in Table 1. Here d_i denotes the size cutoff corresponding to $i\%$.

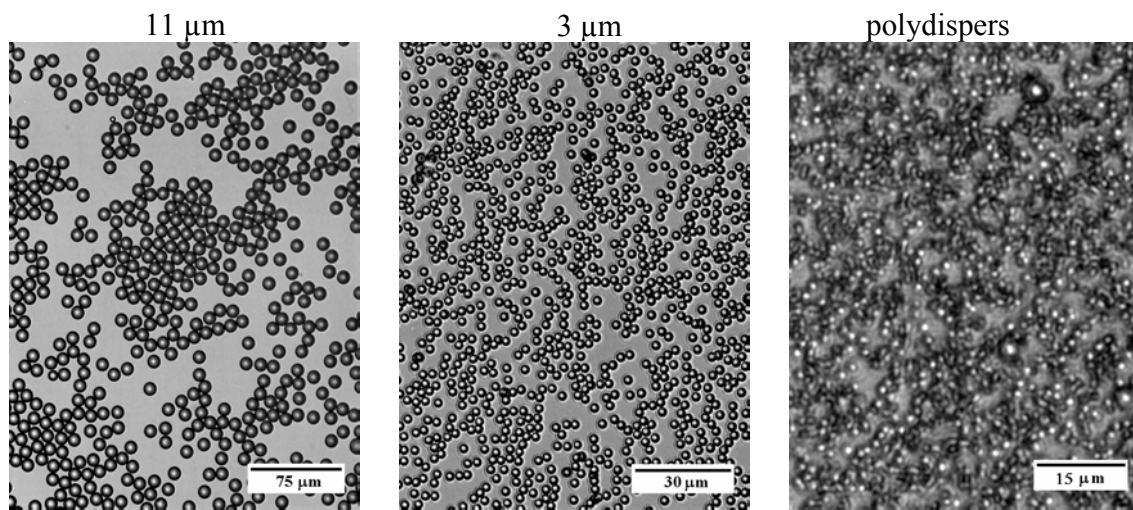


Figure 1. Micrographs of the polystyrene particles

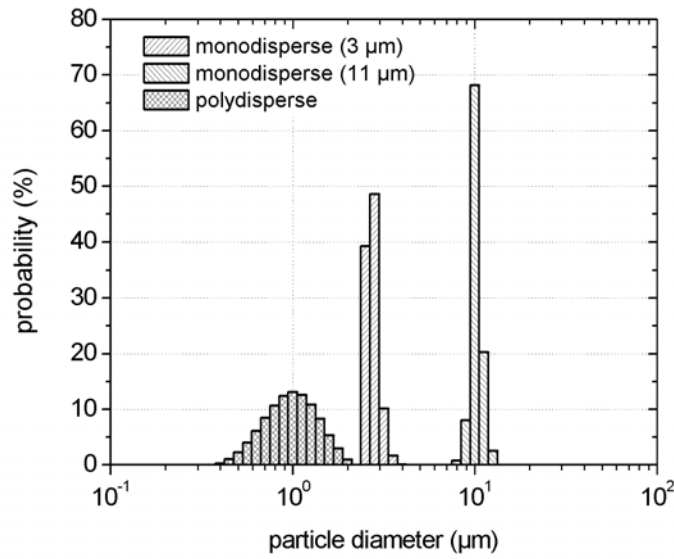


Figure 2. Size distribution of the polystyrene particles

Table 1. Average volume weighted diameter D and normalized polydispersity I of polystyrene particles used in inverse ferrofluids.

Polystyrene Particles	D (μm)	I
Monodisperse 11 μm	10.86	0.143
Monodisperse 3 μm	2.92	0.186
Polydisperse 0.56 – 4.5 μm	1.08	0.873

We utilized the ferrofluid APG 512A (Lot. N° F083094CX from Ferrotec, Co.) which has excellent long term stability. It contains magnetite particles dispersed in synthetic hydrocarbon. The ferrofluid has a density of 1.23 g/cm^3 and a viscosity of 116 mPa s at a temperature of $20 \text{ }^\circ\text{C}$, at which the measurements of the shear modulus have been performed. The magnetization curve obtained in a SQUID magnetometer is displayed in Fig. 3. The data were fitted according to Ref [14] by

$$M(H) = \phi_F M_F \frac{\int_0^{\infty} a^3 g(a, D_F, s_F^2) L\left(a^3 \frac{\pi \mu_0 M_F H}{6 k_B T}\right) da}{\int_0^{\infty} a^3 g(a, D_F, s_F^2) da} \quad (11)$$

where we are assuming that a lognormal distribution $g(a, D_F, s_F^2) = \frac{1}{a s_F \sqrt{2\pi}} \exp\left(\frac{-\ln^2(a/D_F)}{2s_F^2}\right)$ describes the polydispersity of the ferrofluid, as e.g. reported in Ref. [15]. In Eq (11) ϕ_F denotes the volume fraction of the active magnetic material in the ferrofluid and M_F the saturation magnetization of bulk magnetite, a is the diameter of the magnetic particles, and L the Langevin function. The lognormal distribution is characterized by the parameters D_F and s_F . The first is defined via $\ln D_F = \langle \ln x \rangle$, the latter describes the mean deviation of $\ln x$ from its mean value. The fit is shown in Fig. 3 by the solid curve. It makes use of **three** fit parameters which are listed in the inset. The initial susceptibility was obtained as the initial slope of the fitted curve. The corresponding initial permeability is $\mu_r = 1.96$. The saturation magnetization is estimated from the fitted parameters to $M_S = \phi_F M_F = 27.2$ kA/m.

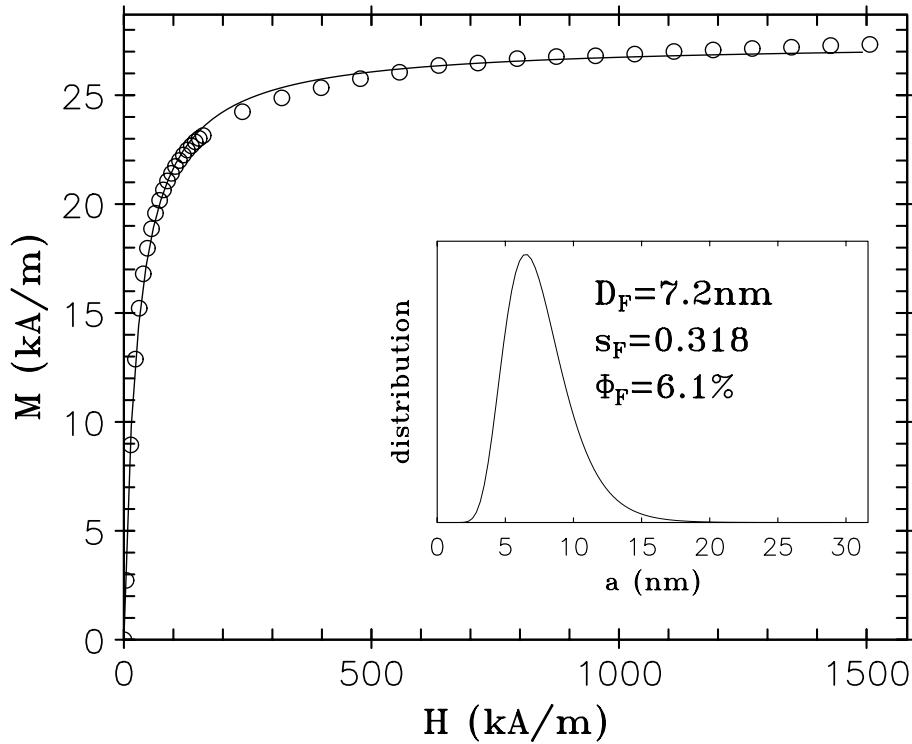


Figure 3. Magnetization curve of the ferrofluid APG 512A, denoted by open circles. The solid line is a fit of Eq. (11) to this data, **utilizing a domain magnetization of $M_F=446$ kA/m** [2]. The inset displays the parameters and the size distribution of the magnetic particles obtained from this fit.

3.2 Sample preparation. The inverse ferrofluids were prepared by dispersing different amounts of dried polystyrene particles in the ferrofluid. The system was alternately stirred for 10 to 15 minutes and sonicated for the same time until a homogeneous mixture was obtained. The volume fractions of non-magnetic particles, namely $\phi_V = 0.175, 0.250$ and 0.300 , were determined from mass calculations. All three volume fractions have been used for the three different particle sizes of polystyrene. The obtained magnetic fluids have been proven to be stable against sedimentation for ten hours as investigated by means of a radiosopic measurements of the homogeneity of the particle distribution [16].

3.3 Rheological measurements. A rotational rheometer (MCR500, Anton Paar) with the commercial magnetorheological device (MRD) and a coaxial parallel plate system with a diameter of 20 mm (PP 20/MR) was used. The distance between the plates was adjusted to 0.3 mm in order to optimize the sensitivity. Viscoelastic properties of ferrofluids were measured using the “magneto sweep” method, described in Ref. [17]. It performs a measurement of G' and G'' under oscillatory shear at constant frequency and constant amplitude, while logarithmically increasing the magnetic field strength. During the measurement, the field is oriented perpendicular to the plates of the rheometer, and thus, perpendicular to the direction of the flow. In order to ensure that the structure is not destroyed, oscillatory measurements were carried out in the linear viscoelastic range. The linearity was checked by varying the strain amplitude on the samples. The measurements were then performed at constant strain amplitude $\gamma = 0.01\%$ and constant oscillatory frequency $\omega = 10$ rad/s. The magnetic field strength was increased logarithmically from 1 to 274 kA/m. Each of the rheological measurements was performed with a freshly prepared sample at 20 °C.

3.4 Optical observations. A long distance microscope (QUESTAR QM100) was used to observe the structure of inverse ferrofluids which are placed between two glass plates of area 70 x 25 mm and separated 25 μm apart from each other. We take the advantage of the large working distance of this microscope to place the sample within a pair of Helmholtz coils in order to apply a homogeneous magnetic field strength to the sample.

4. Results and discussion

4.1 Chain patterns. The pattern of the polystyrene particles emerging after a magnetic field is applied are shown in Fig. 4 for three different suspensions. The individual particles can only be resolved clearly for the largest diameter, but the chain formation can clearly be seen in all three samples. The chains are not isolated ones; due to chain-chain interaction they rather form a network with a complicated structure which is not captured by the idealized theory [10].

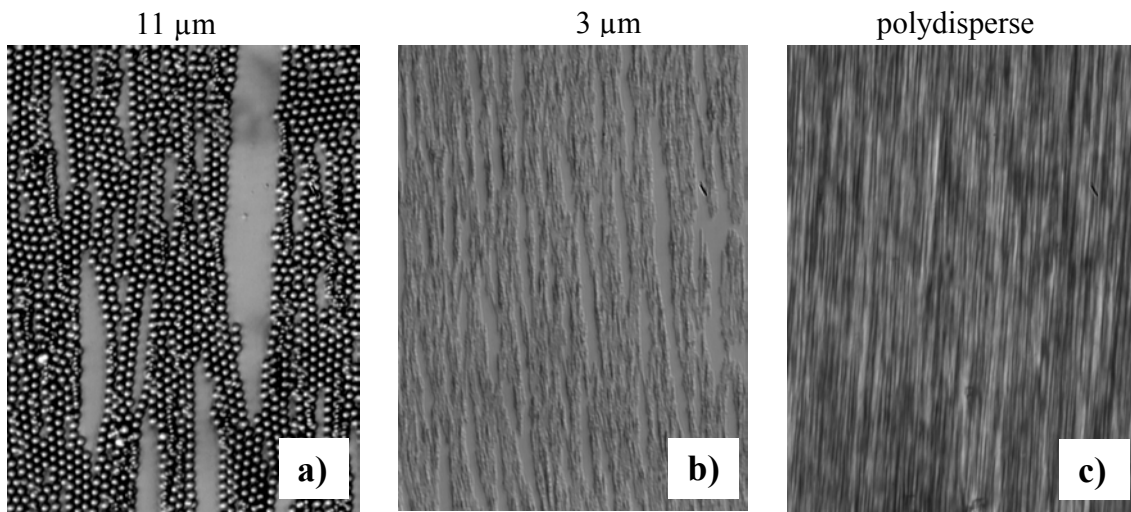


Figure 4. Structures forming in inverse ferrofluids with $\phi_V = 0.175$ of nonmagnetic particles obtained with a long distance microscope. The magnetic field strength $H = 41.4$ kA/m was applied. The field of view is 400×600 μm .

The chains shown in Fig. 4 are indeed expected for the magnetic fields applied there. According to Eqs. (4-8) one can calculate the magnetic field H_g which is necessary to ensure that 99% of the chains are gap spanning in our measuring system. The results are shown in Table 2. Obviously H_g for monodisperse particles is smaller than 1 kA/m whereas all our measurements have been performed for fields larger than 1 kA/m. In this way we can expect that all chains are gap spanning in the whole range of the magnetic field investigated. The situation is more complicated, of course, for polydisperse particles where the differences in sizes could break the continuity of the chains and probably not all of them are really gap spanning.

TABLE 2. The magnetic field strength H_g calculated for all the samples used in this paper. For polydisperse particles we indicate the H_g according to the mean diameter in brackets for comparison.

D	N_{gap}	ϕ_V	H_g (kA/m)
10.86 μm	30	0.175	0.03
		0.250	0.03
		0.300	0.03
2.92 μm	100	0.175	0.24
		0.250	0.24
		0.300	0.24
1.08	202	0.175	(1.12)
		0.250	(1.11)
		0.300	(1.11)

4.2 Rheological results. Next we investigate the rheological properties of the suspensions. Fig. 5 displays the storage modulus (G') and the loss modulus (G'') as a function of magnetic field strength H for different volume fractions and particle sizes. Here the columns of plots have been measured for constant particle size, and the rows for constant volume fraction. As we can observe for all measurements, the magneto sweep shows an intersection of the curves for the loss modulus and the storage modulus, indicating a transition from a more liquid-like behavior with $G' < G''$ to a more solid-like behavior with $G' > G''$. This transition can be understood by an increase of the magnetic forces with the magnetic field: The particle-particle forces become stronger in the chains, thus G' overcomes G'' for sufficiently large fields. For weak fields the magnetostatic forces are small compared to the hydrodynamic forces.

The transition from liquid- to solid-like behavior is affected by the volume fraction of non-magnetic particles. Increasing the volume fraction ϕ_V from 0.175 to 0.250 (first to second row in Fig. 5), the intersection is shifted in all columns considerably to larger magnetic fields. This shift is in agreement with Eq. (10) where the storage modulus is proportional to the volume fraction. However, a further increase to $\phi_V = 0.300$ has the opposite effect: the crossover point is slightly shifted to the left again.

Such a reverse effect has also been observed in measurements of the yield stress [18] at similar ϕ_V . It can be attributed to the considerable dilution of the ferrofluid by the high volume fraction of nonmagnetic particles. For such high concentrations the ferrofluid can no longer be regarded as an embedding fluid for the particles, and thus the magnetic forces exerted by the ferrofluid decreases. Eq. (10) ceases to be valid.

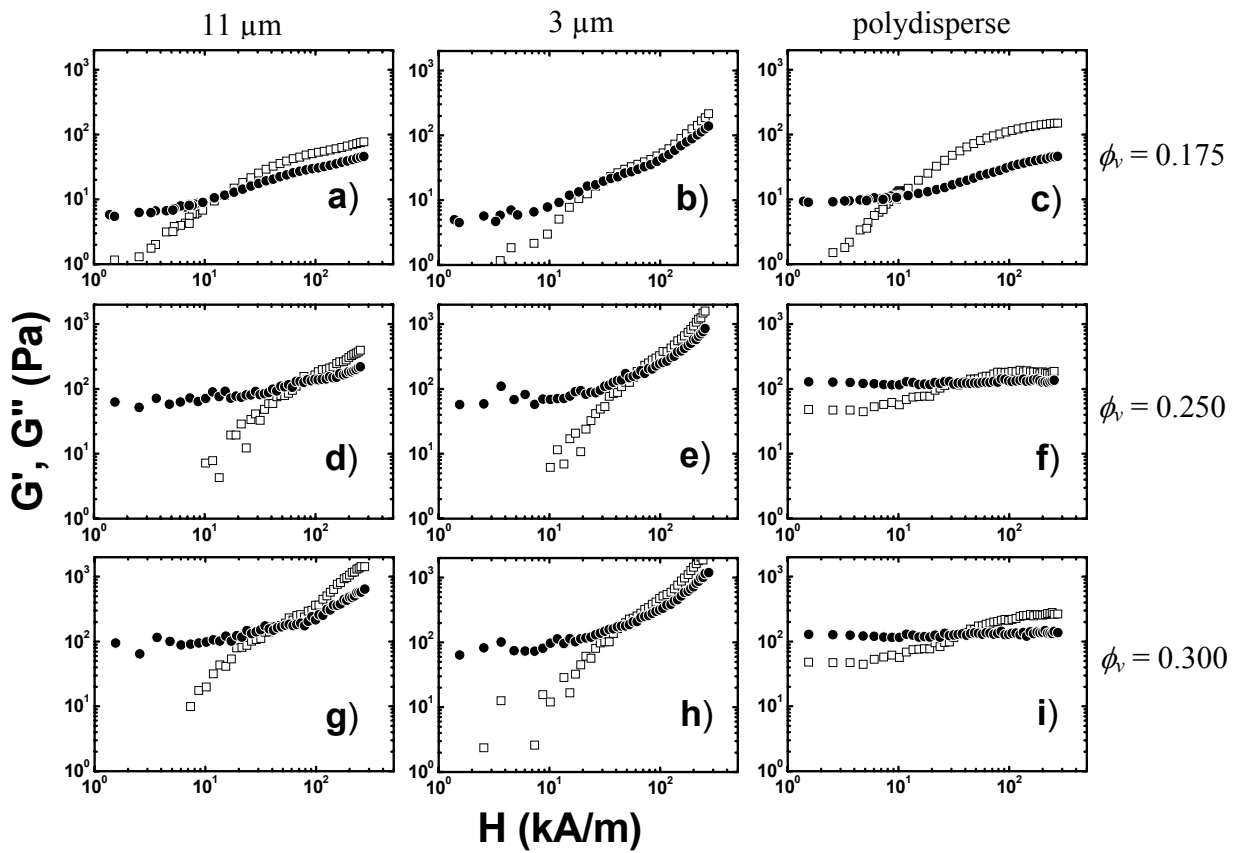


Figure 5. Magneto sweep curves showing the storage modulus G' (\square) and the loss modulus G'' (\bullet) of the inverse ferrofluids as a function of magnetic field strength for different volume fraction ϕ_V and particle mean diameter D of the non-magnetic particles.

Next we address the influence of the particle size on the moduli. If we compare the oscillatory measurements for 11 and 3 μm , we observe that there are no prominent changes. This confirms that G' is independent of the particle size as is predicted by Eqs. (9, 10).

On the other hand, the particle size distribution has a strong effect on the viscoelastic response. The right side column of Fig. 5 displays the magneto sweep plots for a ferrofluid with polydisperse non-magnetic particles. For these particles the storage modulus G' increases more slowly with the magnetic field than for the monodisperse ones. This is valid for all the volume fractions studied. Moreover, the curves show a plateau, indicating that the viscoelastic properties are no longer affected by the influence of the magnetic field. A similar effect has also been found in rotational tests for magnetorheological fluids made with polystyrene particles containing inclusions of magnetite. The flow curve for polydisperse particles was situated well beyond the curve for monodisperse particles [19].

4.3 Comparison with theory. Fig. 6 shows the storage modulus data as a function of the volume fraction, particle size and field strength made dimensionless according to the theory of de Gans *et al.* for the linear regime [10]:

$$\tilde{G}' = G' / \frac{3}{4} \mu_0 \mu_r \beta^2 \zeta(4) \phi_v M_s^2 \left[2 \left(1 + \frac{\beta \zeta(3)}{2} \right)^{-2} + \left(1 - \frac{\beta \zeta(3)}{4} \right)^{-2} \right] \quad (12)$$

Here G' represents the experimental data and M_s is the saturation magnetization. The scaled magnetic field is defined by $\tilde{H} = H / M_s$. Figures 5 a), b), and c) give a comparison of experiment and theory for the volume fractions $\phi_v = 0.175, 0.250$ and 0.300 , respectively. In the first two plots, the experimental data for monodisperse particles (denoted by circles and triangles) are found to be located in the vicinity of the diagonal, which represents the theory.

Taking into account that this model contains considerable simplifications (the structure of the suspension at rest is that of straight, gap spanning isolated chains parallel to the field; and chain-chain interactions are neglected) the agreement with this theory in the linear regime is good, and even better

than in Ref. [10]. Here it is important to mention that equation (12) is only valid for the linear magnetic regime which, in our case is found to be up to $H = 5$ kA/m ($\tilde{H}^2 = 0.03$). However, as we can see in Fig. 6, our data are in accordance with the model by de Gans *et al.* [10] for up to $\tilde{H}^2 \sim 1.5$, which corresponds to $H = 33.4$ kA/m. According to the magnetization curve of the ferrofluid in Fig. 3, for this value of the magnetic field the magnetization curve can still be approximated linearly with a standard deviation of 1.9 kA/m, i.e. the linear approximation is fairly good. This could be the reason why we found good agreement for our experiments in an extended range. When H approaches the saturation, the theory is no longer valid so that the experimental data in Fig. 6 for $\tilde{H}^2 > 10$ deviate from the diagonal.

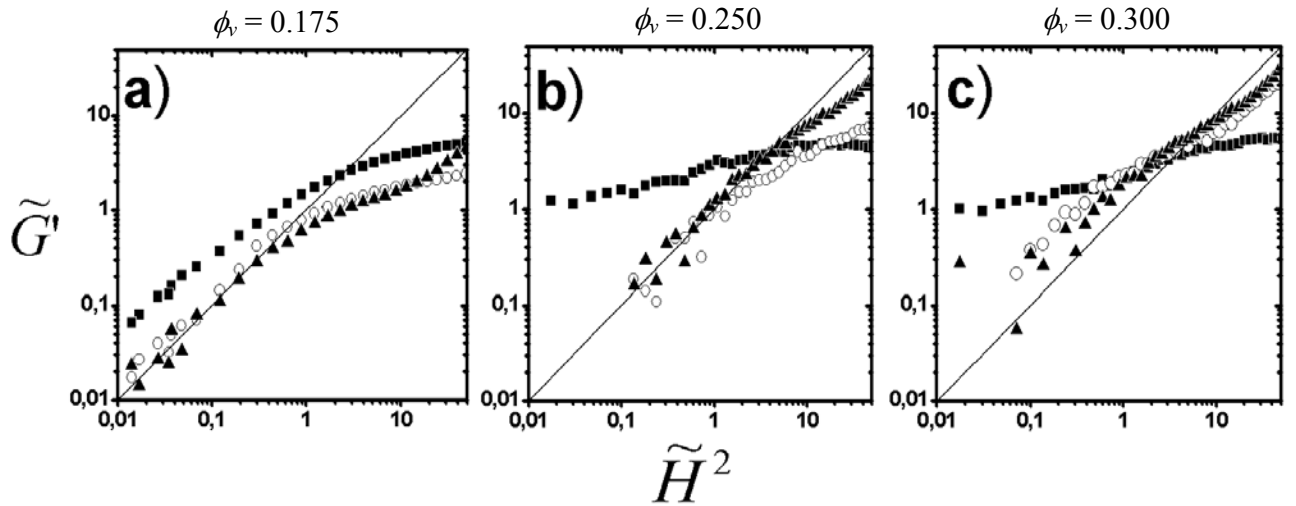


Figure 6. Storage modulus scaled according to Eq. (12) for inverse ferrofluids containing polystyrene monodisperse particles with 3 μm (\circ) and 11 μm (\blacktriangle), and polydisperse (\blacksquare) ones. The diagonal line represents the theory.

The convincing agreement observed for low and medium volume fractions does not hold true for $\phi_v = 0.300$. In Fig. 6 c), the experimental data exceed the predictions of the theory. However, the monodisperse particles keep the same tendency of the theory in the linear range. The increase of the storage modulus might be explained by the chain-chain interactions, which have not been considered in the theory.

In all three plots of Fig. 6 the results for polydisperse particles deviate considerably from the predictions. In the linear regime of the magnetization we observe an enhanced storage modulus in comparison with the monodisperse particles, while it is weakened for stronger magnetic fields. We believe that for weak magnetic fields and high concentrations the enhanced stiffness must be explained by non-magnetic interactions, which are not included in the theory.

The effect that polydisperse particles might weaken the chains, as observed for higher values of the magnetic field, has recently been predicted in theoretical studies for a bidisperse model ferrofluid, and was termed “poisoning effect” [20]. It has been confirmed in molecular dynamics simulations for chain formation in standard ferrofluids [4]. There it is emphasized that the small particles “change the effective magnetic permeability of the background for the large particles, and thus diminish the effective dipolar interaction between them”. This “poisoning effect” might also play a role for the nonmagnetic particles in inverse polydisperse ferrofluids discussed in this paper.

5. Conclusions

We have investigated the linear viscoelasticity of inverse ferrofluids made by dispersing polystyrene particles in the micrometer range. The studies are carried out by magneto sweep tests under variation of particle size and volume fraction of nonmagnetic particles. For monodisperse particles of sufficiently low concentration we found a convincing quantitative agreement with a recently proposed model of linear viscoelasticity by de Gans *et al.* The normalized storage modulus follows the predictions for the linear regime of the magnetization even in an extended range. In particular, the storage modulus increases with the volume fraction, but does not depend on the particle size. The agreement is remarkable, because the assumption of single isolated chains, which are *not interacting*, was not valid: We could observe the alignment of chains via microscopy.

However, the value and applicability of this model to “real worlds” polydisperse magnetorheological fluids seems limited: For an inverse ferrofluid with polydisperse particles no quantitative agreement could be found, certainly a consequence of the simplifying assumptions of the model. Moreover, we

found that the storage modulus of the higher concentrated polydisperse fluid increased only marginal with the magnetic field. This slow increase can be attributed partly to the enhanced hydrodynamic interaction at high concentrations and small fields, whereas at high fields the “poisoning effect” may be responsible for the weaker storage modulus of the polydisperse suspensions compared to the monodisperse ones. This “poisoning effect” was recently observed in molecular dynamic calculations for polydisperse particles in ferrofluids. However, a simulation for magnetorheological fluids, which have no permanent dipoles, is still missing.

Acknowledgements:

The authors wish to thank G. Jena for help with the rheological measurements. Clarifying discussions with H. R. Brand, Ch. Gollwitzer, R. Krauß, and A. Müller are gratefully acknowledged. R. S. G. acknowledges a stipend from the DAAD and CONACYT, and support by project B9 of SFB 481.

References

- [1] J. Popplewell, R.E. Rosensweig, and J.K. Siller, *J. Magn. Magn. Mater.* **149**, 53 (1995).
- [2] R.E. Rosensweig, *Ferrohydrodynamics*, (Cambridge University Press, 1985).
- [3] S. Odenbach, *Magnetoviscous Effects in Ferrofluids*, (Springer 2002); and references therein.
- [4] Zuwei Wang and Christian Holm, *Physical Review E* **68**, 041401 (2003)
- [5] A.T. Skjeltorp, *Phys. Rev. Lett.* **51**, 2306 (1983).
- [6] D.J. Klingenberg, C.F. Zukoski, *Langmuir* **6**, 15 (1990).
- [7] R.E. Rosensweig, *J. Rheol.* **39**, 179 (1995).
- [8] J.E. Martin and R.E. Anderson, *J. Chem. Phys.* **104**, 4814 (1995).

-
- [9] G. Bossis, E. Lemaire, O. Volkova, and H. Clerex, *J. Rheol.* **41**, 687 (1997).
- [10] B.J. De Gans, C. Blom, A. P. Philipse, and J. Mellema, *Phys. Rev. E*, **60**, 4518 (1999).
- [11] B.J. De Gans, N.J. Duin, D. van den Ende, and J. Mellema, *J. Chem. Phys.* **113**, 2032 (2000).
- [12] B.E. Kashevsky, W.I. Kordonsky, and I.W. Prokhorov, *Magnetohydrodynamics* **3**, 368 (1988).
- [13] J. Popplewell and R. E. Rosensweig, *J. Phys. D: Appl. Phys.* **29**, 2297 (1996).
- [14] J. Embs, H.W. Müller, C. E. Krill, F. Meyer, H. Natter, B. Müller, S. Wiegand, M. Lücke, R. Hempelmann, and K. Knorr, *Magnetohydrodynamics* **37**, 222 (2001).
- [15] M. Rasa, *Eur. Phys. J. E* **2**, 265 (2000).
- [16] R. Richter and J. Bläsing, *Review of Scientific Instruments* **72**, 1729 (2001).
- [17] K. Wollny, J. Läger and S. Huck, *Appl. Rheol.* **12**, 25 (2002).
- [18] O. Volkova and G. Bossis, *J. Rheol.* **44**, 91 (2000).
- [19] E. Lemaire, A. Meunier, and G. Bossis, *J. Rheol.* **39**, 1011 (1995).
- [20] S. S. Kantorovich, *J. Magn. Magn. Mater.* **258 – 259**, 471 (2003).